Chain elongation in continuous microbial electrosynthesis cells: The effect of pH and precursors supply

Journal of CO2 Utilization 83 (2024) 102789

Contents lists available at ScienceDirect

Journal of CO2 Utilization

journal homepage: www.elsevier.com/locate/jcou

Chain elongation in continuous microbial electrosynthesis cells: The effect of pH and precursors supply

Cesar Quintela [a], Pantelis Bountzis [a], Babak Rezaei [b], Chaeho Im [c], Oskar Modin [d], Yvonne Nygård [c,1], Lisbeth Olsson [c], Ioannis V. Skiadas [a], Hariklia N. Gavala [a,*]

[a] Department of Chemical and Biochemical Engineering, Technical University of Denmark, Kgs. Lyngby 2800, Denmark
[b] National Centre for Nano Fabrication and Characterization, DTU Nanolab, Technical University of Denmark, Kgs. Lyngby 2800, Denmark
[c] Division of Industrial Biotechnology, Department of Life Sciences, Chalmers University of Technology, Gothenburg, Sweden
[d] Division of Water Environment Technology, Department of Architecture and Civil Engineering, Chalmers University of Technology, Gothenburg, Sweden

ARTICLE INFO

Keywords:
Microbial electrosynthesis
Chain elongation
Butyric acid
Caproic acid
pH

ABSTRACT

Microbial electrosynthesis (MES) enables the production of carbon-neutral chemicals using CO_2 as a carbon source. Acetic acid is the main MES product, but recent studies show the direct production of elongated carboxylic acids, e.g., butyric and caproic acid. However, the production of elongated acids in MES systems is still inefficient due to the low growth rates of acetogenic bacteria and to limited solventogenic rates. Subsequently, researchers have produced elongated carboxylic acids directly from acetic acid or have operated MES systems at low pH to favor solventogenesis. However, the effect the addition of different chain elongation precursors and the operation pH exerts in the bioelectrochemical production of elongated acids remains unclear. To investigate this, three pH-controlled MES systems were operated in this study with continuous liquid and gas supply. MES systems elongating acetic acid at pH 6 achieved higher butyric (0.71 vs. 0.42 g L^{-1}) and caproic acid (0.71 vs. 0.42 g L^{-1}) titers in the absence of CO_2 sparging. Additionally, lowering the pH to 5 in the MES systems fed with CO_2 and acetic acid improved the elongated acids titers, reaching 0.72 g L^{-1} butyric and 0.33 g L^{-1} caproic acid. The 16 S rRNA analysis showed the community was dominated by Oscillibacter at pH 6, and by Clostridium at pH 5. Furthermore, the first scanning electron microscopy pictures revealing biofilm stratification in MES cathodes were taken in this study, where homogeneous rod-shaped bacteria biofilm layers, in contact with the graphite cathode, were covered by heterogeneous biofilm layers.

1. Introduction

Anthropogenic CO_2 emissions have been confirmed to be the main driver of global warming and associated adverse impacts on climate change [1,2]. To limit cumulative CO_2 emissions and climate warming, all industries and economies must reach an average carbon neutrality. Models predict a temperature increase above 1.5° (where irreversible climate changes start) from pre-industrial levels to occur before the end of the century, while modeled pathways limiting the temperature increase below this boundary imply immediate CO_2 emissions reduction already in this decade [3]. The chemical industry sector has a great potential to contribute to the reduction of carbon emissions, since most chemicals are still produced from fossil fuels [3]. Microbial Electro-Synthesis (MES) is one of the technologies that could aid in decarbonizing the chemical industry, as it uses renewable electricity to convert CO_2 emissions into low-carbon-footprint chemicals. This can be done using acetogenic microbes as catalysts, which can uptake electrons from the cathode of an MES cell to reduce CO_2 into acetic acid through the Wood-Ljungdahl pathway (reaction 1). The concept was first demonstrated by Nevin et al. [4] using a pure culture of *Sporomusa ovata* and by Marshall et al. [5] using a mixed culture.

$$2CO_2 + 8e^- + 8H^+ \rightarrow C_2H_3O_2^- + H^+ + 2H_2O \quad (1)$$

So far, acetic acid is the main product of microbial electrosynthesis, but significant efforts have been made in the last decade to expand the product portfolio and target higher-value compounds. Elongating the carboxylic acid chain of acetic acid by MES was first proven successful in batch systems to produce butyric and caproic acid [6]. In 2015, Ganigué

* Corresponding author.
E-mail addresses: hnga@kt.dtu.dk, hari_gavala@yahoo.com (H.N. Gavala).
[1] Present address - VTT Technical Research Centre of Finland, Espoo, Finland.

https://doi.org/10.1016/j.jcou.2024.102789
Received 16 January 2024; Received in revised form 10 April 2024; Accepted 22 April 2024
Available online 30 April 2024

et al. [7] demonstrated the bioelectrochemical production of butyric acid directly from CO_2. Later, in 2018, Jourdin et al. [8] achieved the first continuous production of caproic acid from CO_2. The elongation of carboxylic acids chains takes place through the reverse beta-oxidation pathway, using lactic acid, ethanol, or methanol as electron donors. In MES, it has been suggested that acetic acid is first reduced to ethanol (also termed solventogenesis, reaction 2), which is then used as the electron donor by reverse beta-oxidizers to elongate acetic acid into first butyric (reaction 3) and then caproic acid (reaction 4) [7,8].

$$C_2H_3O_2^- + 5H^+ + 4e^- \rightarrow C_2H_6O + H_2O \quad (2)$$

$$6C_2H_6O + 4C_2H_3O_2^- \rightarrow 5C_4H_7O_2^- + H^+ + 4H_2O + 2H_2 \quad (3)$$

$$6C_2H_6O + 5C_4H_7O_2^- \rightarrow 5C_6H_{11}O_2^- + C_2H_3O_2^- + H^+ + 4H_2O + 2H_2 \quad (4)$$

Despite improvements in reactor design and electrode configuration, acetogenic growth and ethanol production as an intermediary are still the main limitations for the bioelectrochemical production of butyric and caproic acids from CO_2 [9]. In some studies, researchers have supplied both acetic acid and CO_2 to the systems to avoid the acetogenic growth limitations [6,10,11]. However, the effect of CO_2 and acetic acid in the process has, until now, gained less attention. On the other hand, pH is one of the operational conditions affecting both acetogenic and solventogenic rates [12,13]. At low pH, the undissociated fraction of the carboxylic acids, which can cross the bacterial membrane and then dissociate at the higher intracellular pH, increases. This results in the cell spending energy in proton transport to the outside of the membrane, thus lowering the growth yield [14]. To prevent this, solventogenesis is promoted at low pH to reduce the concentration of carboxylic acids [15,16], and therefore, MES operation at low pH could potentially address the limiting ethanol production step in bioelectrochemical chain elongation processes. However, the reverse beta-oxidation pathway also increases the number of acid molecules, as more ethanol than acid is used as substrate for chain elongation to result in a positive energy yield, and this translates into a higher number of acids in the product side of the reaction (reactions 3 and 4). Additionally longer-chain fatty acids exhibit higher hydrophobicity, which also increases the diffusion of the acids into the cell [17]. Therefore, the chain elongation reaction is usually also inhibited at low pH [18]. Despite the importance and complexity of the pH effect in the bioelectrochemical production of butyric and caproic acid from CO_2 and/or acetic acid, the MES performance at different pH in pH-controlled MES systems has not yet been elucidated.

In this study, three H-type MES cells were used to investigate strategies to enhance the production of butyric and caproic acid from CO_2 and acetic acid. The MES were run continuously, with a constant supply of fresh catholyte and gas, while the cell voltage, catholyte pH, and temperature were controlled. The overall performance of MES targeting the production of butyric and caproic acid was studied by focusing on two main parameters: the addition of chain elongation precursors (i.e., CO_2, acetic acid, and butyric acid) and pH. Additionally, 16 S rRNA and SEM analyses were performed to characterize the suspended and biofilm communities. It was observed that both the addition of chain elongation precursors and the operation using lower pH (pH 5 vs. pH 6) promoted the formation of chain-elongated products. Furthermore, the addition of acetic acid to MES fed with CO_2 decreased CO_2 consumption, and chain elongation was shown to be more efficient in MES not sparged with CO_2, suggesting the redundancy of inorganic carbon addition in the bioelectrochemical chain elongation of acetic acid. Finally, microbial analysis showed that different microbial communities were responsible for the chain elongation observed at pH 6 and pH 5, the latter and most efficient being dominated by *Clostridium* spp. Moreover, the SEM pictures revealed two distinct communities within the cathodic biofilm: a homogeneous microbial community in contact with the cathode, covered by layers of a different and more diverse community.

2. Materials and methods

2.1. Culture medium

The catholyte of the MES cells was a modified basal anaerobic (BA) medium, containing the necessary nutrients for microbial growth. Stock solutions were prepared as described by Grimalt-Alemany [19]: 1) macronutrients solution (NH_4Cl, 100 g L^{-1}; NaCl, g L^{-1}; $MgCl_2 \bullet 6\ H_2O$, 10 g L^{-1}; $CaCl_2 \bullet 2\ H_2O$, 5 g L^{-1}), 2) dipotassium hydrogen phosphate solution ($K_2HPO_4 \bullet 3\ H_2O$, 200 g L^{-1}), 3) sodium sulphate solution (Na_2SO_4, 100 g L^{-1}), 4) sodium sulphide solution (Na_2S, 24.975 g L^{-1}), 5) vitamin solution (biotin, 10 mg L^{-1}; folic acid, 10 mg L^{-1}; pyridoxine HCl, school 50 mg L^{-1}; riboflavin HCl, 25 mg L^{-1}; thiamine HCl, 25 mg L^{-1}; cyanocobalamin, 0.5 mg L^{-1}; nicotinic acid, 25 mg L^{-1}; p-aminobenzoic acid, 25 mg L^{-1}; lipoic acid, 25 mpg L^{-1}; d-pantothenic acid hemicalcium salt, 25 mg L^{-1}), and 6) modified ATCC 1754 trace metal (micronutrients) solution (nitrilotriacetic acid, 2000 mg L^{-1}; $MnSO_4 \bullet H_2O$, 1119 mg L^{-1}; $Fe(SO_4)_2(NH_4)_2 \bullet 6\ H_2O$, 800 mg L^{-1}; $CoCl_2 \bullet 6\ H_2O$, 200 mg L^{-1}; $ZnSO_4 \bullet 7\ H_20$, 200 mg L^{-1}; $CuCl_2 \bullet 2\ H_2O$, 20 mg L^{-1}; $NiCl_2 \bullet 6\ H_20$, 20 mg L^{-1}; $Na_2MoO_4 \bullet 2\ H_2O$, 20 mg L^{-1}; $Na_2SeO_3 \bullet 5\ H_2O$, 27 mg L^{-1}; $Na_2WO_4 \bullet 2\ H_2O$, 25 mg L^{-1}; H_3BO_3, 10 mg L^{-1}; $AlCl_3$, 10 mg L^{-1}).

These stock solutions were added to deionized water to prepare the modified BA medium in the following amounts: macronutrients solution, 20 ml L^{-1}; dipotassium hydrogen phosphate solution, 5 ml L^{-1}; sodium sulphate solution, 10 ml L^{-1}; sodium sulphide solution, 0.2 ml L^{-1}; vitamin solution, 10 ml L^{-1}; and trace metal solution, 10 ml L^{-1}. Finally, yeast extract was supplemented to the media to a final concentration of 0.5 g L^{-1}. The only difference from [19] was a reduction of Na_2S stock solution usage by four times, to achieve a final concentration of 1 ml L^{-1} in the media. This was done to avoid precipitation and darkening of the media and the reactor, which would hinder monitoring of the biofilm formation and OD measurements. In some of the experiments the media was also supplemented with acetic acid (8 g L^{-1} in the media) and butyric acid (3.5 g L^{-1} in the media).

To prepare the anolyte solution only macronutrients, dipotassium hydrogen phosphate, and sodium sulphate solutions were used, at the same concentrations used for the catholyte.

2.2. Configuration of the microbial electrosynthesis cells

Four MES cells (MES1, MES2, MES3, and MES-ab) were designed, mounted, and operated through this study, and the overall configuration is shown in Fig. 1. The water-jacketed, H-type glass bodies of the systems were custom made by Mikrolab (Denmark). The cathodes used were 7.5×3x3 cm graphite blocks, and the anodes were 15×0.5 cm (H x Ø) rods made of IrMMO coated titanium (Magneto Special Anodes, Netherlands). Both were held to the lids with titanium wire (0.81 mm thickness), and connected to a potentiostat (Ivium, Netherlands). Between the anode and cathode chambers, a cation exchange membrane was placed (Membrane International, USA), held in place and sealed by a gasket and a metal clamp. The pH was monitored and controlled by a pH electrode (Mettler Toledo, Switzerland), and a pH transmitter (Knick, Germany) was connected to two pumps for acid (HCl 2 M) and base (KOH 5 M) addition. The temperature was controlled by a water bath (Julabo, Germany) connected to the water jackets of the cathodic and anodic chambers. The gas cylinder was connected to a mass flow controller (Bronkhorst, Netherlands), and the gas was flowing into the cathode chamber through a stainless-steel tube. A peristaltic pump was used to control the rate of liquid media supply through the top lid. Liquid flow out occurred naturally via a level tube. In the cathodic chamber, the catholyte was continuously mixed by a magnetic stirrer. There were sampling ports for liquid sampling in both the cathodic and anodic chamber, and for gas sampling in the cathodic chamber (the anodic chamber headspace was open to the air). The whole MES set-up was placed inside a fumehood.

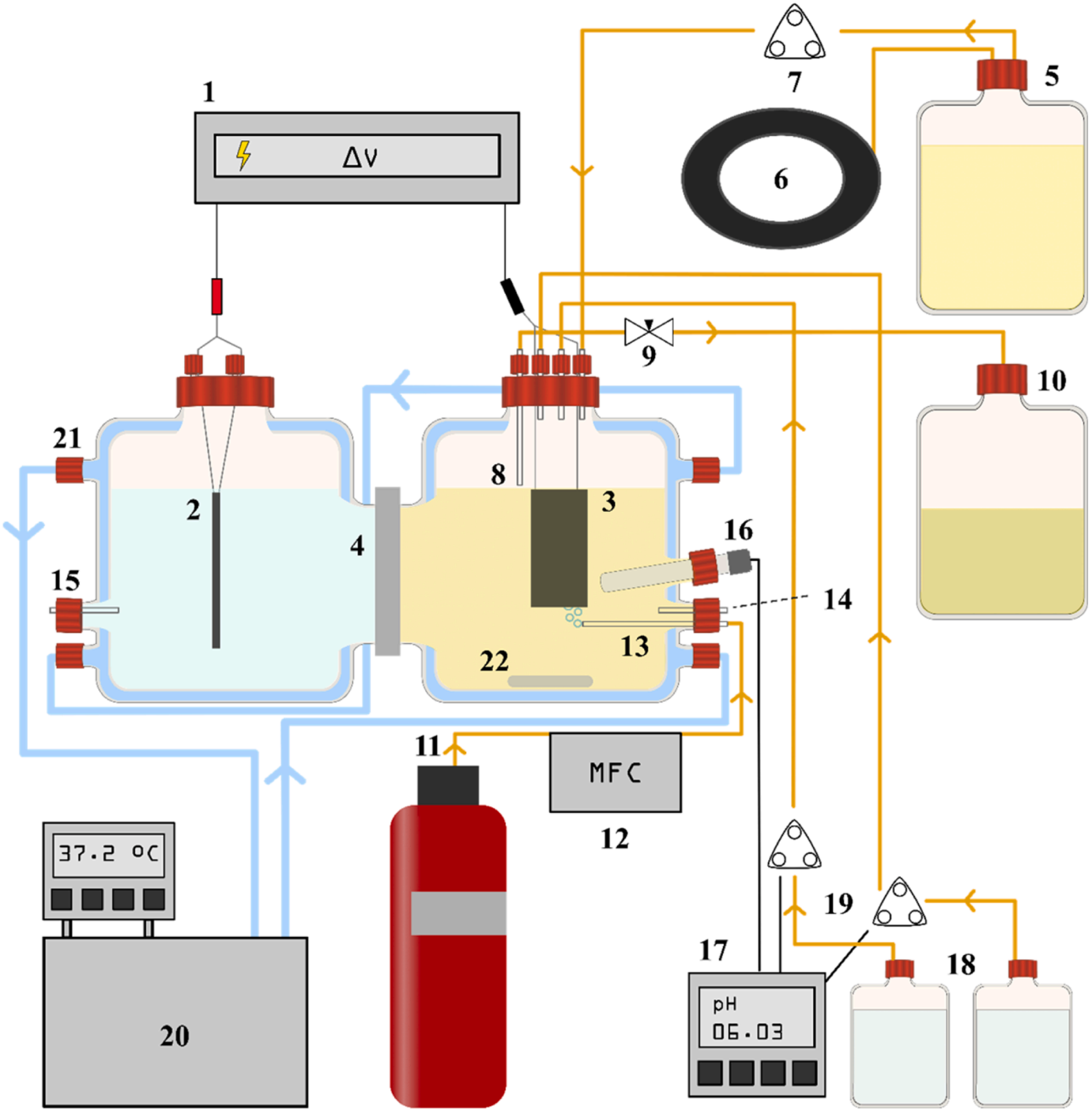

Fig. 1. Flow diagram of the MES cells designed, built, and operated in this study. The main parts of the systems are numbered in the figure and are: (1) potentiostat, (2) anode, (3) cathode, (4) cation exchange membrane, fixed in-between the two chambers with a metal clam, (5) catholyte fresh medium, (6) N_2 bag, (7) liquid inflow peristaltic pump, (8) level / liquid and gas outlet tube, (9) gas sampling port, (10) effluent bottle, (11) gas cylinder, (12) mass flow controller, (13) gas inlet tube, (14) catholyte liquid sampling port, (15) anolyte liquid sampling port, (16) pH electrode, (17) pH transmitter, (18) acid and base solutions, (19) peristaltic pumps for acid and base solutions, (20) water bath, (21) water jacket, (22) magnetic stirring bar. Note: the pH electrode (16), was shown on top of the gas inlet tube (13) for graphic purposes, but the actual location was below the cathode, at the same height as the gas sparger.

2.3. Start-up and operation of the systems

Prior to the start of the MES systems, the cation exchange membrane was first soaked in the anolyte solution overnight. Then the systems were mounted, the anolyte and catholyte solutions were poured into the reactor, and the catholyte was flushed with N_2 for 30 min. The gas flow and composition was then switched to the one used in each MES, the pH, temperature and cell voltage control were connected, and finally the systems were inoculated. The inoculum size for MES1 and MES2 was 50 % of the final catholyte volume, and it was taken from MES3, which was used for running preliminary experiments on the viability of the system and the use of CO_2 and acetic acid as the carbon source at a pH of 6, and an HRT of 7 days. MES3 was originally inoculated using anaerobic digester sludge from the Lyngby-Taarbæk wastewater treatment plant (Denmark). The sludge was heat pre-treated to remove methanogenic bacteria, by subjecting it to 95 °C for 15 min, while being flushed

with N_2. In addition, all inocula were supplemented with anaerobic mixed liquor taken from trickle bed reactors (TBRs) performing syngas fermentation and producing mainly acetic, butyric, and caproic acid [20] to reduce the start-up time needed to enrich an acetogenic and chain elongating mixed community. The origin of the TBRs microbial community was also heat-pretreated anaerobic sludge coming from Lyngby-Taarbæk wastewater treatment plant (Denmark), therefore the enriched strains supplemented with the TBR effluent were already present in the original inoculum.

MES1 and MES2 were operated at the same conditions apart from the gas flow rate, which was 1 ml min^{-1} in MES1 and 0.77 ml min^{-1} in MES2 (the gas flow rate in MES2 was lower than in MES1 due to an, initially, incorrect mass flow controller calibration). MES3 was used for additional experiments with chain elongation precursors addition in the absence of CO_2, and MES-ab was used for abiotic controls. In the MES3 experiments, the system was continuously sparged with N_2, and the flow was controlled using a rotameter. This was done to avoid excessive buildup of H_2 partial pressures, which could affect acetogenic and solventogenic rates and thus distort the CO_2 effect that wanted to be investigated. MES-ab was a new, unused set-up to ensure abiotic conditions, and it was run only for a few days in each condition. Table 1 summarizes the conditions tested in each of the MES systems. The systems were run continuously until a steady state was reached.

During operation, the catholyte was continuously replaced with a peristaltic pump set to a hydraulic retention time (HRT) of 5 days, while the anolyte was fully replaced manually every second week. The temperature of the systems was kept constant at 37° C, and the potentiostat was used to fix a cell voltage of −3.5 V, which in preliminary experiments (using a reference electrode immersed in the catholyte and converting CO_2 to carboxylic acids in MES3) was equivalent to −1.0 V cathode potential.[2] Liquid and gaseous samples from the cathodic chamber were taken three times per week to monitor the reactor performance. The anolyte composition was analyzed every time it was replaced, to include the products, which had potentially migrated to the anolyte through the membrane, in the calculations.

2.4. Analytical methods

The gas composition in the cathodic chamber was determined in a gas chromatograph (8610 C, SRI Instruments, Germany) equipped with a thermal conductivity detector and two packed columns (6′ × 1/8″ Molsieve 13× column and 6′ × 1/8″ silica gel column) connected in series through a rotating valve. The columns were kept at 65°C for 3 min, followed by a 10 °C min-1 ramp till 95°C, and a 24 °C min-1 ramp reaching 140 °C. 50 μl gas samples were collected and injected with a gas-tight syringe (model 1750SL, Hamilton) [21]. Volatile fatty acids and alcohols in the catholyte and anolyte were measured through a High-Performance Liquid Chromatograph (Shimadzu, USA) equipped with a refractive index detector and an Aminex HPX-87 H column (Bio-Rad, Denmark) maintained at 60°C, using as eluent 12 mM H_2SO_4 at a flow rate of 0.6 ml min^{-1}.

The biomass concentration in the catholyte was indirectly monitored by measuring the optical density at a wavelength of 600 nm (OD_{600}) using a spectrophotometer (DR3900, Hach Lange). The pH of the broth was measured externally using a PHM210 pH meter (Hach, USA), that was also used for recalibrating the internal pH electrode when necessary.

Table 1
Conditions tested in each of the different MES used in this study. Conditions not separated by a horizontal line indicates they were tested sequentially, without restarting the system.

System	Condition	Carbon substrate	pH
MES1	CO_2 fermentation	CO_2	6
&	Acetate Addition	CO_2 + Acetate	6
MES2	Acidic pH	CO_2 + Acetate	5
MES3	Acetate elongation	Acetate	6
	Butyrate addition	Acetate + Butyrate	6
MES-ab	Abiotic	CO_2	6
	Abiotic (Acidic)	CO_2	5

[2] Preliminary experiments highlighted the challenge of long-term continuous MES operation including reference electrodes, which would require continuous or periodic replacement of electrolyte solution. Although no reference electrodes were included in the experiments shown in this study, we can assume that the 3.5 V cell voltage would result in cathode potentials close to the 1 V cathode potential obtained in preliminary experiments.

2.5. Calculations

The electron yields, e-yields, represent the portion of the consumed electrons which ended up in our products. The electrons consumed include the electrical current and the available electrons present in the acetic and butyric acid being consumed in the system. The consumption of yeast extract was not added to the e-yield calculations, as its complex and variable composition makes it difficult to estimate the content in available electron equivalents for acetogenesis and chain elongation. An extensive explanation of the e-yield calculation can be found in [22]. In short, to calculate the e-yields (reaction 5), the average production or consumption rate (positive and negative, respectively) of each compound at the steady-state (r_i) was multiplied by the number of electron equivalents in that compound (e_i^-), to obtain the e-mol production/consumption rate for each compound. This was divided by the total e-mol consumption rate ($\sum r_i \bullet e_i^-$) in that steady-state, to calculate the e-yield for each compound. The e-mol consumption due to the electric current was calculated using the real-time monitoring of the current given by the potentiostat. The amperage measured by the potentiostat was converted to e-mol min^{-1} taking into account that one ampere is equivalent to $6.24{\cdot}10^{18}$ electrons per second [23].

$$e - Yield_i = \frac{r_i \bullet e_i^-}{\sum r_i \bullet e_i^-} \quad (5)$$

2.6. Community analysis

For suspended growth samples, 50 ml of culture was collected from the catholyte, centrifuged to remove the supernatant, and the pellet was frozen at −20°C. For the biofilm samples, one side of the graphite blocks was washed with phosphate-buffer saline (PBS) solution and then scratched with a knife to collect all biofilm, which was frozen at −20 °C.

The DNA was extracted using DNeasy Blood and Tissue Kits (Qiagen, Denmark), and submitted to Macrogen Inc. (Korea) for 16 S rRNA amplicon library preparation and sequencing using Illumina Miseq (300 bp paired-end sequencing). The libraries were constructed according to the 16 S Metagenomic Sequencing Library Preparation Protocol (Part #15044223, Rev. B) using Herculase II Fusion DNA Polymerase Nextera XT Index Kit V2. Regions V4-V5 of 16 S rRNA gene were amplified with primers 515 F (5′-GTGYCAGCMGCCGCGGTAA-3′) and 926 R (5′-CCGYCAATTYMTTTRAGTTT-3′) [24].

Raw reads were merged, quality-filtered, and denoised, using the DADA2 algorithm within the Qiime2 pipeline, to obtain ASVs [25]. Taxonomic assignment was then performed using a classify-sklearn algorithm, together with a classifier trained on the Greengenes2 (2022.10) database. Further downstream analysis was performed using phyloseq and ggpubr packages in R. The raw sequences obtained in this study are available in the NCBI SRA database with BioProject accession number PRJNA1063202.

2.7. SEM analysis

The biofilm on the surface of the graphite electrode was primarily fixed for 6 h using a fixative reagent containing 2.5 % glutaraldehyde at 4 °C, followed by washing with a 0.1 M phosphate buffer solution three times. Next, the samples were gradually dehydrated by immersing the electrode for 30 min in successive ethanol solutions with increasing concentrations (50 %, 70 %, 90 % and absolute ethanol). The samples were dried in a vacuum freeze dryer overnight to preserve the structure of the bacteria and prevent collapsing and deformation. Finally, the samples were sputter-coated with gold for 40 sec to avoid charge accumulation and the surface topography of the samples was examined using scanning electron microscopy (SEM, Zeiss Supra VP 40, Carl Zeiss NTS GmbH, Germany) [26].

3. Results and discussion

In this study, three MES systems were used to investigate the feasibility of chain elongation processes using mixed microbial cultures as biocatalysts. Different carbon substrates were supplied (CO_2, acetic, and butyric acid) at two different pH (pH 5 and pH 6), and electrons were provided by the cathode at a constant cell voltage (-3.5 V). Fig. 2 shows the production profile of the three systems through the whole study.

3.1. Chain elongation improvement by precursor addition

Different studies have shown chain elongation from either CO_2 [8, 27], CO_2 and acetic acid [10], or different carboxylic acids [11], but there is a lack of studies analyzing the effect the addition of these different carbon precursors has on the bioelectrochemical production of butyric and caproic acid. Fig. 3A shows the concentration of butyric and caproic acid before and after supplementing acetic acid to two MES systems (MES1 and MES2) performing CO_2 conversion, and before and after supplementing butyric acid to a MES system (MES3) performing acetic acid elongation. MES1 and MES2 showed the same trend, although MES2 had overall lower chain-elongated products due to the lower gas flow received (as mentioned in Section 2.2). Before the supplementation of acetic acid, the systems still exhibited some chain elongation activity; however, butyric and caproic acid were present in very small quantities (0.023 g L^{-1} butyric, 0.015 g L^{-1} caproic in MES1; and 0.019 g L^{-1} butyric, 0.016 g L^{-1} caproic, in MES2). After the supplementation with acetic acid the concentration of butyric acid increased to 0.423 and 0.288 g L^{-1} in MES1 and MES2, respectively; while the concentration of caproic acid increased to 0.062 and 0.033 g L^{-1}, respectively in MES1 and MES. This is a 15–18x increase in butyric and 2–4x increase in caproic acid production. On the other hand, MES3 (Fig. 3A), fed with acetic acid, and without any CO_2 or carbonate addition, exhibited a more efficient chain elongation process, reaching a caproic acid titer of 0.211 g L^{-1}. In a similar way as in MES1 and MES2, the addition of butyric acid increased the concentration of caproic acid over 2x, reaching a final concentration of 0.5 g L^{-1}.

Fig. 3 shows a tendency of higher yields and titers of chain elongated products in the absence of an inorganic carbon source, i.e., CO_2. This cannot possibly be attributed to a buildup of H_2 partial pressure (that

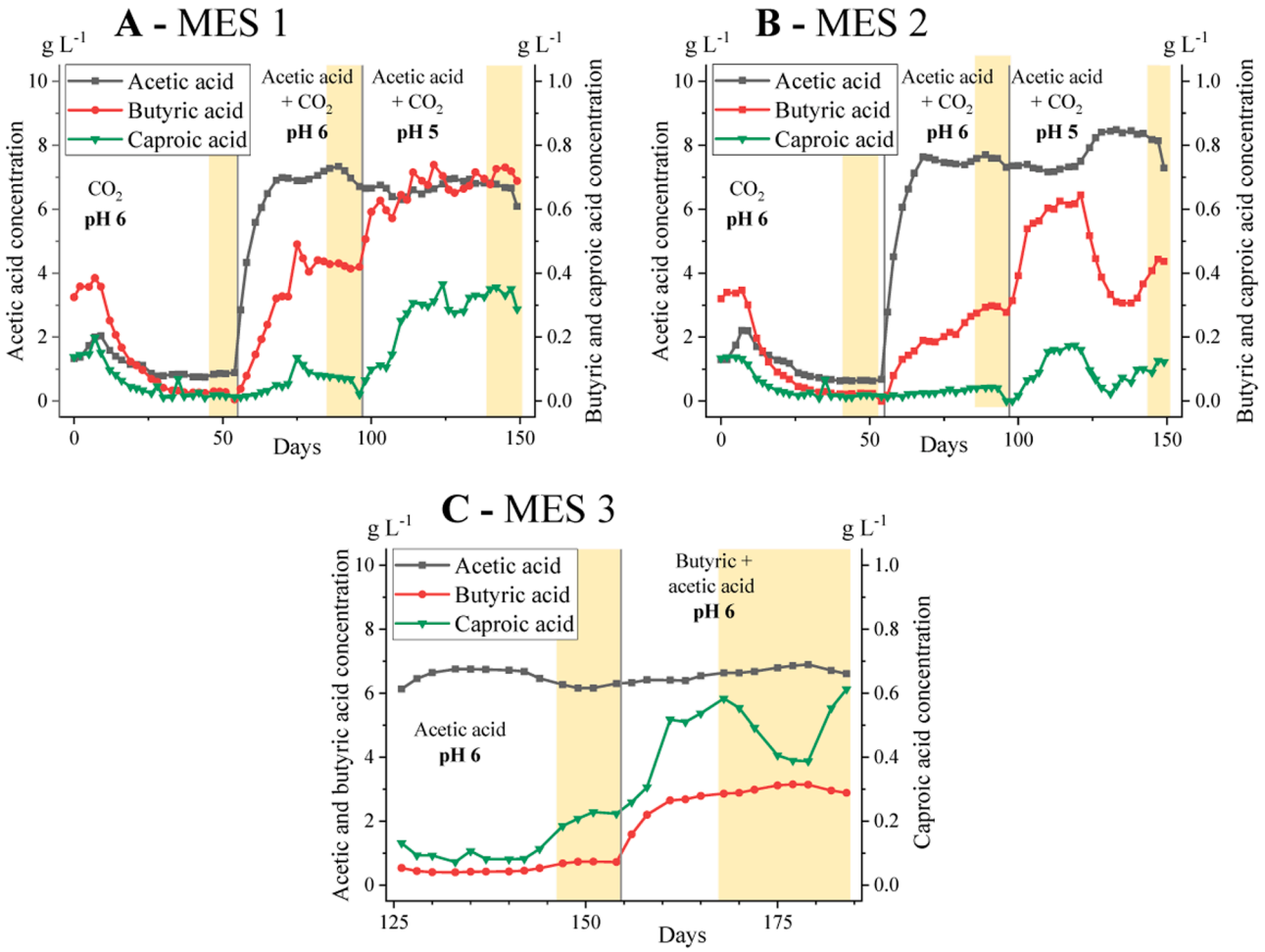

Fig. 2. Main extracellular compounds in MES1 (A), MES2 (B), and MES3 (C). The experimental conditions (pH and carbon addition) are indicated in the graph, and the timeframes considered for the steady-state calculations is highlighted in yellow.

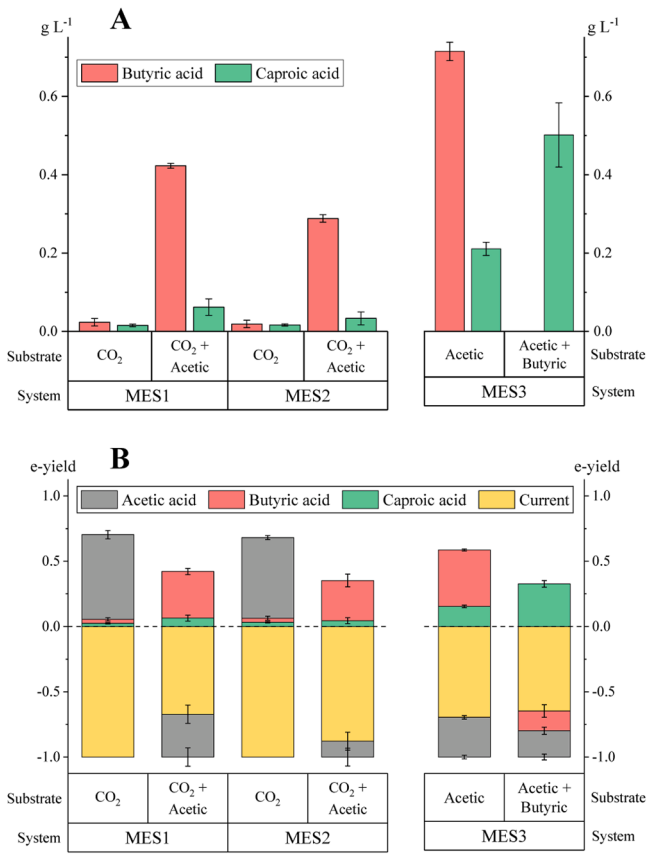

Fig. 3. Concentrations of butyric and caproic acid in the different MES at pH 6 before and after adding a reverse beta-oxidation precursor (A) and e-yields of the different entities participating in reactions 1–4 (B). In MES3, no CO_2 was added to the systems.

could favor solventogenesis, and thus, chain elongation), since a N_2 flow was established to substitute the CO_2 flow and ensure anaerobic conditions. It cannot respond to the longer operation time of MES3 either (150 vs 90 days), as the 90 days in MES1 and MES2 should be sufficient for the development of a steady biofilm. Instead, the absence of inorganic carbon in MES3 could have resulted in the suppression of acetogenesis as a competing pathway for electron use, enhancing thus the transfer of electrons towards the reduction of acetic acid to ethanol and subsequently promoting chain elongation. Similarly, CO_2 has been shown to reduce the yields of butyric and caproic acid in chain elongation studies, by diverting electron equivalents into the acetogenic pathway instead of into the reverse β-oxidation [28]. In the present study ethanol was rarely observed, in agreement with other continuous MES experiments targeting elongated acids [8,10], implying that the rate of ethanol use in chain elongation is higher than the rate of ethanol production. On the other hand, recent studies have suggested that CO_2 is necessary for bacteria chain elongating ethanol [29] and high CO_2 loading rates benefit the elongation of CO_2 [30]. Besides, *C. Kluyveri*, a known chain elongating bacterium, is known to need CO_2 for its protein synthesis [31]. Nevertheless, Raes et al. [11] showed the elongation of acetic, propionic, and butyric acid was possible in three plexiglass MES systems supplied with just 0.25 g L^{-1} ammonium carbonate as inorganic carbon source. Analogously, in this experiment the presence of 0.5 g L^{-1} yeast extract could have allowed the growth of chain elongating bacteria in the absence of CO_2, either by direct consumption or through the CO_2 generated by fermentation of the yeast extract. To the best of our knowledge, this is the first study that compares the bioelectrochemical elongation of acetic acid with and without an inorganic carbon source; and although MES3 lacked a reactor replicate to confirm these findings, the fact that chain elongation was favored in the absence of inorganic carbon source is an outcome that deserves more investigation.

3.2. Chain elongation improvement by acidic conditions

After reaching a steady state converting CO_2 and acetic acid to chain elongated acids, the pH of MES1 and MES2 was changed to 5, based on the hypothesis that a lower pH would enhance ethanol production from acetic acid, and thus improve chain elongation activity, as it was shown in batch MES experiments by Vassilev et al. [27]. Reducing the pH did in fact enhance chain elongation activity (Fig. 4), as both butyric and caproic acid concentration increased in the two MES. Especially, the production of caproic acid increased by 5.4x (MES1) and 3.4x (MES2), reaching concentrations of 0.335 and 0.113 g L^{-1}, respectively, probably due to a significant increase of ethanol production from acetic acid as intermediary. In fact, it can be seen how, especially in MES1, the consumption of acetic acid was enhanced by a lower pH (Fig. 4B). The chain elongation activity reached in MES2 was, especially in this case, lower when compared to MES1 (Fig. 2). This difference was due to disturbances which caused the chain elongation activity to decrease sharply in MES2, resulting in lower concentrations of chain elongated products at the end of the experiment, which did not allow a steady state to be reached. This experiment demonstrates a significant continuous production of chain elongated products from CO_2 and acetic acid at low pH, which reached production rates of 0.142 g L^{-1} day^{-1} butyric and 0.067 g L^{-1} day^{-1} caproic acid. Although most acetic acid was not consumed in this experiment, further tuning of operating conditions such as HRT, cell voltage, and acetic acid concentrations, as well as improvements of the reactor design is needed to optimize acetic acid consumption efficiencies and chain elongation rates. Raes et al. [10] used MES in galvanostatic mode to apply currents about 3x the currents reported in this study (Fig. S1, supplementary material) and produce longer chain carboxylic acids from acetic acid, at pH 5.5 and an HRT of 20 h. Raes et al. obtained lower butyric acid titers (0.59 g L^{-1}), but higher production rates (0.54 g L^{-1} day^{-1}) due to the low HRT used. On the other hand, low HRTs did not allow for significant caproic acid production, which was only detected in trace amounts. Jourdin et al. [8] achieved efficient butyric (3.2 g L^{-1} day^{-1}) and caproic acid (0.95 g L^{-1} day^{-1}) production rates from CO_2 at a pH of 5.8 and an HRT of 4 days, probably due to a very efficient reactor design which maximized the cathodic and membrane surface in respect to the catholyte volume. Nevertheless, the effect of catholyte pH in pH-controlled MES has not been explored before, and as shown in this study, low pH operation would have the potential to further increase the butyric and caproic acid production rates in optimized reactor configurations. However, acidic pH has been showed to increase the toxicity of elongated carboxylic acids [14]. To avoid the inhibition of the undissociated fraction of elongated acids at low pH, in-line extraction of elongated acids could keep their concentrations below toxicity levels [33].

The e-yields, or coulombic efficiencies, calculated for the steady states reached in MES1, MES2, and MES3 (Figs. 3B and 4B) showed that the carboxylic acids produced accounted for 33–70 % of the electrons consumed. Also, no H_2 was detected in the systems during steady-states. The fate of the remaining electrons was to alternative products (5–10 % of electrons), especially propionic, iso-valeric, and iso-butyric, diffusion of carboxylic acids into the anolyte (1–2 % of electrons), reduction of inorganic species such as sulfate, biomass growth, and potentially to the production of non-measured products such as methanol. In this regard, the absence of CO_2 in MES3 improved the e-yields of chain-elongated acids from 42 % and 35 % in MES1 and MES2 (Fig. 3B) to 59 % in MES3. Similarly, decreasing the pH to 5 also improved chain-elongated acids e-yields in MES1 and MES2 to 65 % and 61 %, respectively. Presumably, future designs applying acidic pH in the absence of CO_2 will reach even higher e-yields in chain-elongated acids. This should be combined with studies tuning the acetic acid added in chain-elongating MES, the cell voltage applied, and the HRT to maximize the percentage

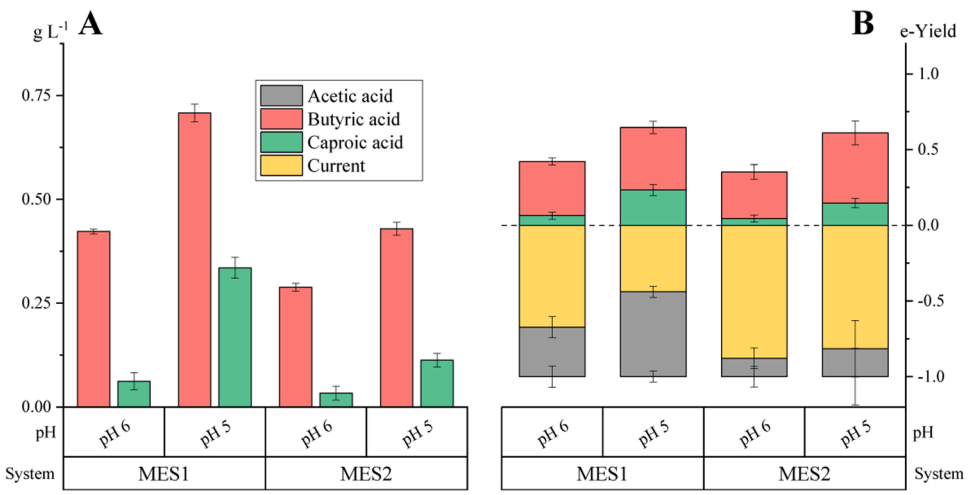

Fig. 4. Concentrations of butyric and caproic acid, in g L^{-1}, in MES1 and MES2 at pH 6 and pH 5 (A); and e-yields of the different entities participating in reactions 1–4 (B).

of acetic acid elongated, the product yields, and the production rates. Decreasing the concentration of acetic acid added may enhance the acetic acid conversion (a maximum of 22 % conversion was achieved in this study) but at the risk of reducing the elongation rates. Additionally, increasing the cell voltage may increase chain elongation rates up to a point, but it will also increase the operational costs. Finally, HRT should be high enough to achieve relevant chain-elongated acid titers without reaching toxicity limits [30]. These fine-tuned parameters can then be implemented in optimized bioelectrochemical designs, which maximize electrode and membrane area to reactor volume ratios and use 3D electrodes to increase the flow of electrons and, thus, volumetric productivities [32].

3.3. Impact of conditions on CO_2 consumption

The CO_2 consumption in all steady states reached in MES1 and MES2 was above the consumption of the abiotic controls (Fig. 5 and table S1). Statistical analysis using 2-way Anova revealed that the addition of acetic acid significantly reduced the consumption of CO_2 in both systems ($p<0.05$), while a reduction of the pH did not decrease CO_2 consumption. Although CO_2 solubility decreases at lower pH values, and this could decrease the CO_2 consumption calculated, the CO_2 consumption percentage did not change in the pH range and the liquid and gas flows used when tested in abiotic controls (table S1, supplementary material). On the other hand, the addition of acetic acid to the media triggered a switch in the electron acceptor in the catholyte from CO_2 to acetic acid, thus reducing acetogenesis. Similarly, the absence of CO_2 in MES3 improved the yields of chain elongated products, presumably as it allowed for more electrons to be directed towards the chain elongation route instead of towards acetogenesis. As it was discussed in previous sections, CO_2 has sometimes been addressed as necessary for chain elongating bacterial growth [29–31]. Interestingly, in this study the reduction in CO_2 consumption when acetic acid was added to the systems was associated with increased chain elongation activity, and the MES3 experiments, which were not sparged with CO_2, exhibited the highest chain elongating activity among the tests performed at pH 6. Nevertheless, the carbon fed to the systems as acetic acid was three times higher than the carbon fed as CO_2, and therefore additional experiments testing different acetic acid: CO_2 ratios should follow before concluding the redundancy of CO_2 in the bioelectrochemical elongation of acetic acid.

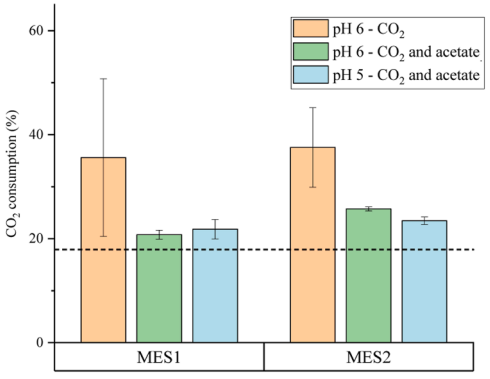

Fig. 5. Consumption of CO_2 as percentage of the total CO_2 fed for each of the steady states reached in MES1 and MES2. The averaged percentage of CO_2 consumed in abiotic controls (Table S1, supplementary material) is indicated with a grey dashed line.

3.4. Microbial community analyses

Samples for 16 S rRNA analysis were taken from MES1 and MES2 at the steady states reached with acetic acid supplementation at pH 6 and pH 5, and the relative abundances were summarized in Fig. 6. The suspended biomass triplicates taken for both MES at pH 6 (each taken on a different date of the steady-state) showed the reproducibility and consistency of the sampling process, as well as of the bacterial community during the steady-state. The relative abundances were also very similar between systems and, although no biofilm samples could be taken from the pH 6 steady-states, at pH 5 the biofilm samples differed only slightly from the attached growth samples. In contrast, there was a notable community shift associated with the pH change. The most abundant genus at pH 6 was *Oscillibacter*, which has been found in other MES communities and has been associated with butyric and caproic acid production [34,35]. On the other hand, at pH 6 there was almost no presence of the *Clostridium_B* genus that was the most abundant genus at pH 5 in both suspended and attached samples. *Clostridium* species are known acetogens and reverse beta-oxidizers and have been detected in MES catholytes and cathodes in several studies [27,35]. *Desulfovibrio* is a known electroactive microbe, which can uptake directly microbes from the cathode [36], however, the fact that it had a significant relative abundance in all liquid samples, but was almost absent from the biofilm samples, could indicate that it was performing other functions such as acetic acid oxidation [37]. *Clostridium* appears to be the key genus responsible for the improved chain elongation at pH 5. Additionally, *Caproicibacter,* another chain-elongating genus, seemed to be especially

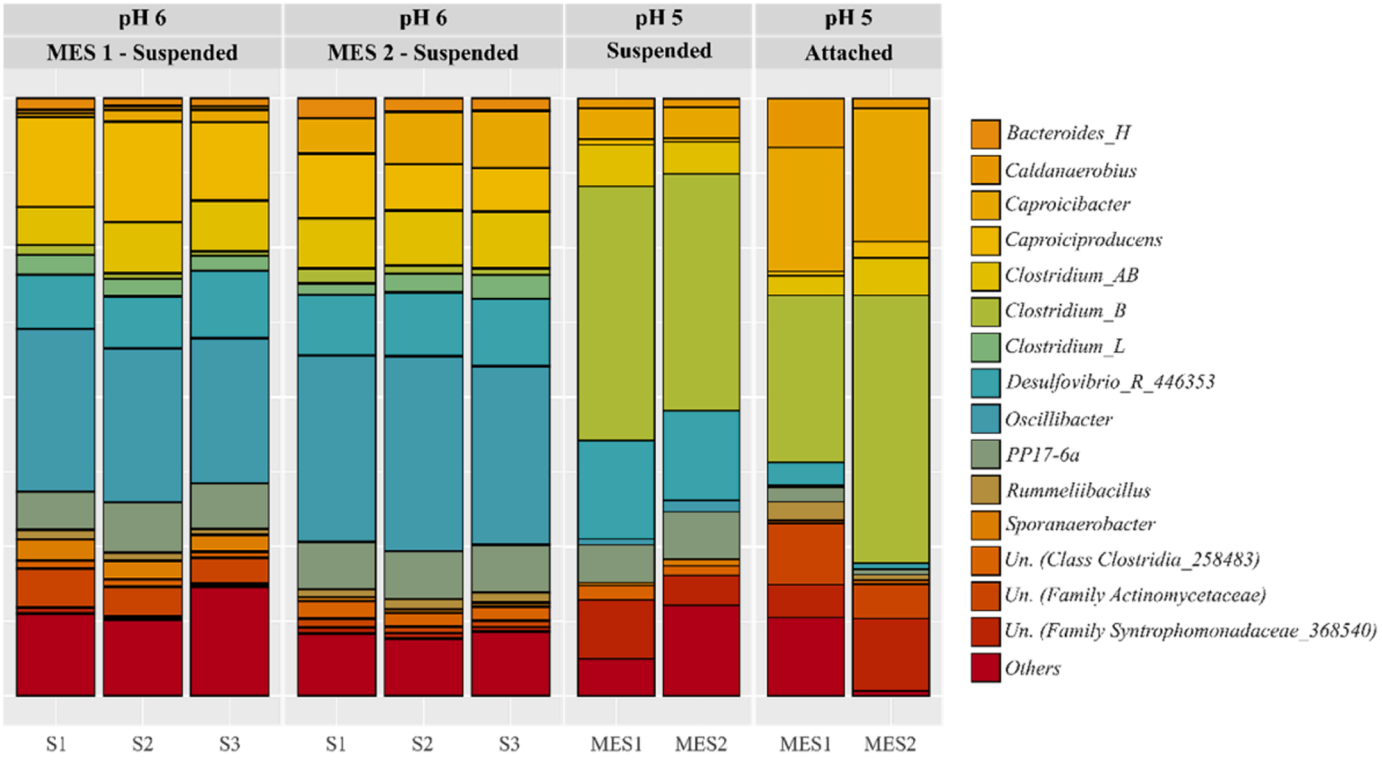

Fig. 6. Relative abundance of the 15 most abundant genera in the pH 6 (CO_2 + acetic acid) and pH 5 steady-states.

abundant in the pH 5 biofilm samples. Nevertheless, although the pH 5 condition had the most efficient chain elongation, both communities were responsible for significant chain elongation using MES. In a similar experiment, La Belle et al. [38] operated batch MES cells at −600 and −800 mV at pH ranging from 4.5 to 6.5 and produced only acetic acid and H_2. In that case, the 16 S rRNA analysis showed that the culture was dominated by *Acetobacterium*, and there was no evidence of *Clostridium*, *Oscillobacter*, or *Caproicibacter* genera. In contrast to the present study, where an inoculum with high diversity was used, La Belle et al. used an inoculum from a previously operated MES systems producing acetic acid, which might have affected the specificity and diversity of the microbial community.

At the end of the study, the cathodic biofilms (Fig. 7A) were fixed, dehydrated, and gold-sputtered to be pictured by the SEM. The biofilm thickness was especially high, and this resulted in a shrinkage of the top layers of the biofilm during the dehydration step (Fig. 7B), which made it possible to photograph the top and bottom layers of the biofilm independently. Consequently, two very distinct communities were detected. At the biofilm bottom (Figs. 7C and 7D), in contact with the cathode surface, only rod-shaped bacteria were seen, which according to the 16 S analysis could correspond to *Clostridium* or *Caproicibacter* genera, both rod-shaped. On the other hand, at the biofilm top layer (Figs. 7E and 7F), a very diverse community was seen, including rod, spherical, and filamentous bacteria of different sizes. Figs. 7G and 7H show simultaneously bottom and top layers of the biofilm. To the best of our knowledge these are the first pictures where a MES cathodic biofilm stratification can be directly observed using SEM. In other studies, in the international literature, SEM is solely used to confirm the cathode nano- or micro-structure and identify the biofilm, which appears as a uniform single or multilayer [8,36,37]. These pictures show how in an open mixed culture MES, operating continuously, the electroactive bacterial layer in contact with the cathode, may end up fully covered by multiple, very diverse, bacterial layers, which might contribute with synergies, but also may generate significant challenges such as mass transfer limitations, and pH, substrates, and products gradients. Further studies should be performed to determine whether this could be a challenge to be addressed in the commercialization of long-term continuous MES systems.

4. Conclusions

In this study, three MES systems were run continuously (concerning both liquid and gas flow) with controlled temperature, cell voltage, and catholyte pH to investigate the influence of pH and different carbon precursors addition (CO_2, acetic acid, and butyric acid) in the production of chain-elongated carboxylic acids. It was shown how the addition of carboxylic acids (acetic and butyric acid) to MES systems fed with CO_2 directed the flow of electron equivalents out of the acetogenic pathway and into the chain elongation route, thus reducing CO_2 consumption but increasing the yield of chain-elongated acids. Similarly, the MES system elongating acetic acid in the absence of CO_2 achieved higher butyric and caproic acid yields than the MES systems fed with acetic acid and CO_2. Therefore, acetic acid and CO_2 act as competing electron acceptors in MES systems, and this should be taken into account in future MES designs to improve the yields of chain-elongated carboxylic acids. Additionally, the reduction of pH from 6 to 5 favored the production of longer-chain fatty acids, presumably as it favored the reduction of acetic acid to ethanol, which was directly consumed for chain elongation. These results correlated with the microbial community analysis, which showed two different communities performing bioelectrochemical chain elongation at pH 6, dominated by *Oscillobacter*, and at pH 5, dominated by *Clostridium*, implying that a more acidic operating pH could lead to changes in the microbial community that translate into more efficient chain elongation processes. At the end of the study, the SEM analyses of the cathode biofilms at pH 5 revealed two distinct communities present in the biofilm: a community of solely rod-shaped bacteria in contact with the cathode covered by a highly diverse bacterial community. This suggests that, in long-term continuous MES systems, the potentially electroactive microbial layer may get covered by a thick biofilm, which reduces their access to nutrients and protons; therefore, maintenance measures may be needed to maintain high productivities over time. Overall, this study points towards the use of MES for the chain

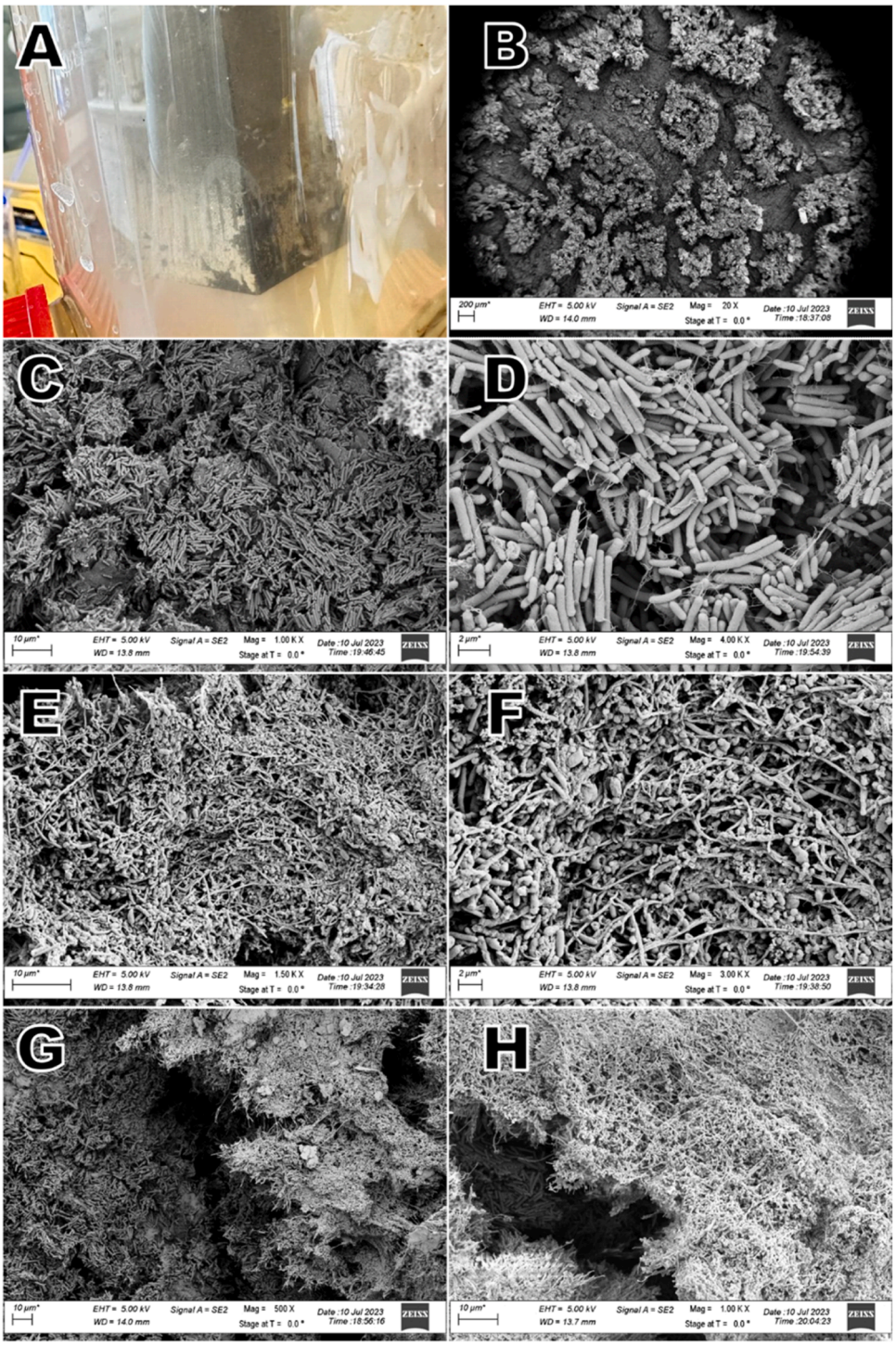

Fig. 7. Visible biofilm in the surface of the MES1 graphite cathode (A) and pictures of the fixed biofilm taken by the scanning electron microscope (B-H). From left to right and top to bottom, 20x magnification picture of the bottom of the cathode, where it can be seen the cracks in the fixed biofilm caused by the shrinkage during the dehydration step (B), 1000x magnification picture of a biofilm crack where bacteria can be seen on the graphite surface (C), 4000x magnification picture of a biofilm crack (D), 1500x (E) and 3000x (F) magnification pictures of the biofilm surface, and 500x (G) and 1000x (H) magnification pictures were both the graphite surface at the bottom and the biofilm surface at the front with their distinct communities can be seen.

elongation of acetic acid effluents at acidic conditions and in the absence of CO_2 as an additional carbon source.

CRediT authorship contribution statement

Ioannis V. Skiadas: Writing – review & editing, Visualization, Supervision, Methodology, Investigation, Conceptualization. **Lisbeth Olsson:** Writing – review & editing, Visualization, Supervision, Methodology, Investigation. **Chaeho Im:** Writing – review & editing, Methodology. **Babak Rezaei:** Writing – review & editing, Methodology, Investigation. **Yvonne Nygård:** Writing – review & editing, Visualization, Supervision, Methodology, Investigation. **Oskar Modin:** Writing – review & editing, Formal analysis, Data curation. **Pantelis Bountzis:** Writing – review & editing, Methodology, Investigation, Formal

analysis, Data curation. **Cesar Quintela Garcia:** Writing – original draft, Visualization, Methodology, Investigation, Formal analysis, Data curation, Conceptualization. **Hariklia Gavala:** Writing – original draft, Visualization, Supervision, Resources, Project administration, Methodology, Funding acquisition, Data curation, Conceptualization.

Declaration of Competing Interest

The authors declare that they have no known competing financial interests or personal relationships that could have appeared to influence the work reported in this paper.

Data Availability

Data will be made available on request.

Acknowledgements

This study was supported by the DTU PhD alliance scheme and DTU Chemical Engineering.

Appendix A. Supporting information

Supplementary data associated with this article can be found in the online version at doi:10.1016/j.jcou.2024.102789.

References

[1] H.O. Pörtner, D.C. Roberts, H. Adams, C. Adler, P. Aldunce, E. Ali, R.A. Begum, R. Betts, R.B. Kerr, R. Biesbroek, Climate change 2022: impacts, adaptation and vulnerability, IPCC, 2022.
[2] P. Arias, N. Bellouin, E. Coppola, R. Jones, G. Krinner, J. Marotzke, V. Naik, M. Palmer, G.-K. Plattner, J. Rogelj, Climate Change 2021: the physical science basis. Contribution of Working Group I to the Sixth Assessment Report of the Intergovernmental Panel on Climate Change; technical summary, (2021).
[3] P.R. Shukla, J. Skea, R. Slade, A. Al Khourdajie, R. Van Diemen, D. McCollum, M. Pathak, S. Some, P. Vyas, R. Fradera, Climate change 2022: Mitigation of climate change, Contribution of Working Group III to the Sixth Assessment Report of the Intergovernmental Panel on Climate Change 10 (2022) 9781009157926.
[4] K.P. Nevin, T.L. Woodard, A.E. Franks, Z.M. Summers, D.R. Lovley, Microbial electrosynthesis: Feeding microbes electricity to convert carbon dioxide and water to multicarbon extracellular organic compounds, MBio 1 (2010), https://doi.org/10.1128/mBio.00103-10.
[5] C.W. Marshall, D.E. Ross, E.B. Fichot, R.S. Norman, H.D. May, Electrosynthesis of commodity chemicals by an autotrophic microbial community, Appl. Environ. Microbiol 78 (2012) 8412–8420, https://doi.org/10.1128/AEM.02401-12.
[6] M.C.A.A. Van Eerten-Jansen, A. Ter Heijne, T.I.M. Grootscholten, K.J. J. Steinbusch, T.H.J.A. Sleutels, H.V.M. Hamelers, C.J.N. Buisman, Bioelectrochemical production of caproate and caprylate from acetate by mixed cultures, ACS Sustain Chem. Eng. 1 (2013) 513–518, https://doi.org/10.1021/sc300168z.
[7] R. Ganigué, S. Puig, P. Batlle-Vilanova, M.D. Balaguer, J. Colprim, Microbial electrosynthesis of butyrate from carbon dioxide, Chem. Commun. 51 (2015) 3235–3238, https://doi.org/10.1039/c4cc10121a.
[8] L. Jourdin, S.M.T. Raes, C.J.N. Buisman, D.P.B.T.B. Strik, Critical biofilm growth throughout unmodified carbon felts allows continuous bioelectrochemical chain elongation from CO2 up to caproate at high current density, Front Energy Res. 6 (2018), https://doi.org/10.3389/fenrg.2018.00007.
[9] N. Chu, W. Hao, Q. Wu, Q. Liang, Y. Jiang, P. Liang, Z.J. Ren, R.J. Zeng, Microbial electrosynthesis for producing medium chain fatty acids, Engineering 16 (2022) 141–153, https://doi.org/10.1016/j.eng.2021.03.025.
[10] S.M.T. Raes, L. Jourdin, C.J.N. Buisman, D.P.B.T.B. Strik, Continuous long-term bioelectrochemical chain elongation to butyrate, ChemElectroChem 4 (2017) 386–395, https://doi.org/10.1002/celc.201600587.
[11] S.M.T. Raes, L. Jourdin, C.J.N. Buisman, D.P.B.T.B. Strik, Bioelectrochemical chain elongation of short-chain fatty acids creates steering opportunities for selective formation of n-butyrate, n-valerate or n-caproate, ChemistrySelect 5 (2020) 9127–9133, https://doi.org/10.1002/slct.202002001.
[12] R. Blasco-Gómez, S. Ramió-Pujol, L. Bañeras, J. Colprim, M.D. Balaguer, S. Puig, Unravelling the factors that influence the bio-electrorecycling of carbon dioxide towards biofuels, Green. Chem. 21 (2019) 684–691, https://doi.org/10.1039/c8gc03417f.
[13] C. Im, K. Valgepea, O. Modin, Y. Nygård, Clostridium ljungdahlii as a biocatalyst in microbial electrosynthesis – effect of culture conditions on product formation, Bioresour. Technol. Rep. 19 (2022), https://doi.org/10.1016/j.biteb.2022.101156.
[14] J.B. Russell, D.B. Wilson, Why are ruminal cellulolytic bacteria unable to digest cellulose at low pH? J. Dairy Sci. 79 (1996) 1503–1509.
[15] J.J. Baronofsky, J.A. Schreurs, E.R. Kashket, Uncoupling by Acetic Acid Limits Growth of and Acetogenesis by Clostridium thermoaceticum, 1984. ⟨https://journals.asm.org/journal/aem⟩.
[16] Y. He, C. Cassarini, P.N.L. Lens, Bioethanol production from H2/CO2 by solventogenesis using anaerobic granular sludge: effect of process parameters, Front Microbiol. 12 (2021), https://doi.org/10.3389/fmicb.2021.647370.
[17] L.R. Jarboe, L.A. Royce, P. Liu, Understanding biocatalyst inhibition by carboxylic acids, Front Microbiol. 4 (2013), https://doi.org/10.3389/fmicb.2013.00272.
[18] R. Ganigué, P. Sánchez-Paredes, L. Bañeras, J. Colprim, Low fermentation pH is a trigger to alcohol production, but a killer to chain elongation, Front Microbiol. 7 (2016) 702, https://doi.org/10.3389/FMICB.2016.00702/BIBTEX.
[19] A. Grimalt-Alemany, C. Etler, K. Asimakopoulos, I.V. Skiadas, H.N. Gavala, ORP control for boosting ethanol productivity in gas fermentation systems and dynamics of redox cofactor NADH/NAD+under oxidative stress, J. CO2 Util. 50 (2021), https://doi.org/10.1016/j.jcou.2021.101589.
[20] Quintela C, (2023) Mixed-culture gas fermentation to butyric and caproic acid in continuous systems: synergies and competitions. PhD thesis, DTU Chemical Engineering, published by the Technical University of Denmark.
[21] A. Grimalt-Alemany, M. Łężyk, L. Lange, I.V. Skiadas, H.N. Gavala, Enrichment of syngas-converting mixed microbial consortia for ethanol production and thermodynamics-based design of enrichment strategies, Biotechnol. Biofuels 11 (2018), https://doi.org/10.1186/s13068-018-1189-6.
[22] K. Asimakopoulos, H.N. Gavala, I.V. Skiadas, Biomethanation of syngas by enriched mixed anaerobic consortia in trickle bed reactors, Waste Biomass-.-. Valoriz. 11 (2020) 495–512, https://doi.org/10.1007/s12649-019-00649-2.
[23] A.J. Bard, L.R. Faulkner, Introduction and overview of electrode processes, Electrochem. Methods.: Fundam. Appl. (2001) 1–43.
[24] W. Walters, E.R. Hyde, D. Berg-Lyons, G. Ackermann, G. Humphrey, A. Parada, J. A. Gilbert, J.K. Jansson, J.G. Caporaso, J.A. Fuhrman, Improved bacterial 16S rRNA gene (V4 and V4-5) and fungal internal transcribed spacer marker gene primers for microbial community surveys, MSystems 1 (2016) e00009–e00015.
[25] E. Bolyen, J.R. Rideout, M.R. Dillon, N.A. Bokulich, C.C. Abnet, G.A. Al-Ghalith, H. Alexander, E.J. Alm, M. Arumugam, F. Asnicar, Y. Bai, J.E. Bisanz, K. Bittinger, A. Brejnrod, C.J. Brislawn, C.T. Brown, B.J. Callahan, A.M. Caraballo-Rodríguez, J. Chase, E.K. Cope, R. Da Silva, C. Diener, P.C. Dorrestein, G.M. Douglas, D. M. Durall, C. Duvallet, C.F. Edwardson, M. Ernst, M. Estaki, J. Fouquier, J. M. Gauglitz, S.M. Gibbons, D.L. Gibson, A. Gonzalez, K. Gorlick, J. Guo, B. Hillmann, S. Holmes, H. Holste, C. Huttenhower, G.A. Huttley, S. Janssen, A. K. Jarmusch, L. Jiang, B.D. Kaehler, K.Bin Kang, C.R. Keefe, P. Keim, S.T. Kelley, D. Knights, I. Koester, T. Kosciolek, J. Kreps, M.G.I. Langille, J. Lee, R. Ley, Y. X. Liu, E. Loftfield, C. Lozupone, M. Maher, C. Marotz, B.D. Martin, D. McDonald, L.J. McIver, A.V. Melnik, J.L. Metcalf, S.C. Morgan, J.T. Morton, A.T. Naimey, J. A. Navas-Molina, L.F. Nothias, S.B. Orchanian, T. Pearson, S.L. Peoples, D. Petras, M.L. Preuss, E. Pruesse, L.B. Rasmussen, A. Rivers, M.S. Robeson, P. Rosenthal, N. Segata, M. Shaffer, A. Shiffer, R. Sinha, S.J. Song, J.R. Spear, A.D. Swafford, L. R. Thompson, P.J. Torres, P. Trinh, A. Tripathi, P.J. Turnbaugh, S. Ul-Hasan, J.J. J. van der Hooft, F. Vargas, Y. Vázquez-Baeza, E. Vogtmann, M. von Hippel, W. Walters, Y. Wan, M. Wang, J. Warren, K.C. Weber, C.H.D. Williamson, A. D. Willis, Z.Z. Xu, J.R. Zaneveld, Y. Zhang, Q. Zhu, R. Knight, J.G. Caporaso, Reproducible, interactive, scalable and extensible microbiome data science using QIIME 2, 2019 37:8, Nat. Biotechnol. 37 (2019) 852–857, https://doi.org/10.1038/s41587-019-0209-9.
[26] J. Li, D. Chen, G. Liu, D. Li, Y. Tian, Y. Feng, Construction of a new type of three-dimensional honeycomb-structure anode in microbial electrochemical systems for energy harvesting and pollutant removal, Water Res. 218 (2022), https://doi.org/10.1016/j.watres.2022.118429.
[27] I. Vassilev, P.A. Hernandez, P. Batlle-Vilanova, S. Freguia, J.O. Krömer, J. Keller, P. Ledezma, B. Virdis, Microbial electrosynthesis of isobutyric, butyric, caproic acids, and corresponding alcohols from carbon dioxide, ACS Sustain Chem. Eng. 6 (2018) 8485–8493, https://doi.org/10.1021/acssuschemeng.8b00739.
[28] C. Quintela, E. Peshkepia, A. Grimalt-Alemany, Y. Nygård, L. Olsson, I.V. Skiadas, H. Gavala, Waste and Biomass Valorization Excessive ethanol oxidation versus efficient chain elongation processes, Waste Biomass. Valoriz. (2023), https://doi.org/10.1007/978-1-4612-1072.
[29] M. Roghair, T. Hoogstad, D.P.B.T.B. Strik, C.M. Plugge, P.H.A. Timmers, R. A. Weusthuis, M.E. Bruins, C.J.N. Buisman, Controlling ethanol use in chain elongation by CO2 loading rate, Environ. Sci. Technol. 52 (2018) 1496–1506, https://doi.org/10.1021/acs.est.7b04904.
[30] L. Jourdin, M. Winkelhorst, B. Rawls, C.J.N. Buisman, D.P.B.T.B. Strik, Enhanced selectivity to butyrate and caproate above acetate in continuous bioelectrochemical chain elongation from CO2: steering with CO2 loading rate and hydraulic retention time, Bioresour. Technol. Rep. 7 (2019), https://doi.org/10.1016/j.biteb.2019.100284.
[31] N. Tomlinson, H.A. Barker, Carbon dioxide and acetate utilization by Clostridium kluyveri: I. Influence of nutritional conditions on utilization patterns, J. Biol. Chem. 209 (1954) 585–595.
[32] L. Jourdin, S. Freguia, V. Flexer, J. Keller, Bringing high-rate, CO2-based microbial electrosynthesis closer to practical implementation through improved electrode design and operating conditions, Environ. Sci. Technol. 50 (2016) 1982–1989, https://doi.org/10.1021/acs.est.5b04431.
[33] P. Batlle-Vilanova, R. Ganigué, S. Ramió-Pujol, L. Bañeras, G. Jiménez, M. Hidalgo, M.D. Balaguer, J. Colprim, S. Puig, Microbial electrosynthesis of butyrate from carbon dioxide: production and extraction, Bioelectrochemistry 117 (2017) 57–64, https://doi.org/10.1016/j.bioelechem.2017.06.004.

[34] Y. Zhang, J. Li, J. Meng, X. Wang, A cathodic electro-fermentation system for enhancing butyric acid production from rice straw with a mixed culture, Sci. Total Environ. 767 (2021), https://doi.org/10.1016/j.scitotenv.2021.145011.
[35] P. Dessì, C. Sánchez, S. Mills, F.G. Cocco, M. Isipato, U.Z. Ijaz, G. Collins, P.N. L. Lens, Carboxylic acids production and electrosynthetic microbial community evolution under different CO2 feeding regimens, Bioelectrochemistry 137 (2021), https://doi.org/10.1016/j.bioelechem.2020.107686.
[36] C.W. Marshall, D.E. Ross, K.M. Handley, P.B. Weisenhorn, J.N. Edirisinghe, C. S. Henry, J.A. Gilbert, H.D. May, R.S. Norman, Metabolic reconstruction and modeling microbial electrosynthesis, Sci. Rep. 7 (2017), https://doi.org/10.1038/s41598-017-08877-z.
[37] M. del Pilar Anzola Rojas, R. Mateos, A. Sotres, M. Zaiat, E.R. Gonzalez, A. Escapa, H. De Wever, D. Pant, Microbial electrosynthesis (MES) from CO2 is resilient to fluctuations in renewable energy supply, Energy Convers. Manag 177 (2018) 272–279, https://doi.org/10.1016/j.enconman.2018.09.064.
[38] E.V. LaBelle, C.W. Marshall, J.A. Gilbert, H.D. May, Influence of acidic pH on hydrogen and acetate production by an electrosynthetic microbiome, PLoS One 9 (2014), https://doi.org/10.1371/journal.pone.0109935.